Journal of Polymers and the Environment
https://doi.org/10.1007/s10924-023-02981-0

ORIGINAL PAPER

Properties of PLA-co-PBSu Copolymers Rapidly Synthesized by Reactive Processing

Zoi Terzopoulou[1] · Alexandra Zamboulis[1] · Nikolaos D. Bikiaris[1] · Antigoni Margellou[2] · Miguel Angel Valera[3] · Ana Mangas[3] · Savvas Koltsakidis[4] · Konstantinos Tsongas[4,5] · Dimitrios Tzetzis[4] · Konstantinos Triantafyllidis[2]

Accepted: 22 June 2023

Abstract

This work describes the synthesis of poly(lactic acid) by the ring-opening polymerization of L-lactide in the presence of oligo(butylene succinate) with two different molecular weights (M_n = 6100 and 16300 g/mol) as a macroinitiator during reactive processing. The macroinitiators were added in concentrations 1 wt%, 2.5 wt%, 5 wt%, 10 wt% and 15 wt% in respect to the L-lactide mass in the premix. The properties of the received copolymers were extensively studied with spectroscopic techniques, GPC, DSC, XRD, TGA as well as nanoindentation. Blocky copolymers were received with number average molecular weights ranging from 30 to 100 kg/mol, which decreased with increasing the PBSu content in the feed. The introduction of the flexible PBSu chains decreased the single glass transition detected, while DSC and XRD gave indications that both components crystallized in the copolymers with PBSu premix content > 5 wt%. Thermal stability was maintained and depended on the composition and molecular weight. Nanoindentation showed that despite the decreasing trend of hardness and elastic modulus with increasing PBSu content, the PLA-PBSu 2.5% copolymers had simultaneously higher elasticity modulus and strength compared to the other compositions, possibly because of a complementary effect of their high molecular weight and crystallinity. These copolymers were promising for production with continuous reactive extrusion, a novel, fast and economically viable method to commercially produce PLA-based polymers.

Keywords Biobased polyester · Poly(lactic acid) · Poly(butylene succinate) · Reactive processing · Copolymers

Introduction

The continuous accumulation of plastic waste and depletion of fossil resources has led the European Union (E.U.) to support the development of biobased plastics through research funding, and publish directives on plastic bags and single-use plastics [1]. In 2022, revisions to the EU legislation on Packaging and Packaging Waste were proposed, aiming to reduce its use, promote reuse and increase the recycling rates. At the same time, these new rules will redefine biobased, biodegradable and composting plastics, ensuring they actually contribute towards a sustainable future [2].

Poly(lactic acid) (PLA) is a biobased thermoplastic polyester that currently dominates the sustainable plastics field, with ever-growing production capacities and applications [3–8]. Depending on the chiral isomer used (D or L lactide), it can be either semicrystalline or amorphous, and most of the commercially available PLA intended for commodity applications, such as packaging and single-use products, is

✉ Zoi Terzopoulou
terzozoi@chem.auth.gr

1 Laboratory of Polymer and Colors Chemistry and Technology, Department of Chemistry, Aristotle University of Thessaloniki, 54124 Thessaloniki, Greece

2 Laboratory of Chemical and Environmental Technology, Department of Chemistry, Aristotle University of Thessaloniki, 54124 Thessaloniki, Greece

3 AIMPLAS, Asociación de Investigación de Materiales Plásticos Y Conexas, Carrer de Gustave Eiffel, 4, 46980 Paterna, Valencia, Spain

4 Digital Manufacturing and Materials Characterization Laboratory, School of Science and Technology, International Hellenic University, 14 Km Thessaloniki, 57001 N. Moudania, Greece

5 Department of Industrial Engineering and Management, International Hellenic University, 57001 Thessaloniki, Greece

Published online: 26 July 2023

poor in D-lactide (2–10 mol%). PLA should not be considered biodegradable because of it is very slow degradation rate, but it is compostable in industrial composting conditions. PLA also suffers from slow crystallization kinetics and inherent brittleness, which are often controlled with the use of additives, addition of a second component (blends), or comonomers [6, 9–15].

Another important biobased compostable thermoplastic polyester that is available in the market is poly(butylene succinate) (PBSu). PBSu is synthesized by the melt polycondensation of succinic acid and 1,4-butanediol, both monomers that are obtained from renewable sources. While possessing excellent crystallization ability, melt processability and chemical resistance, medium molecular weight PBSu can be brittle with a low elastic modulus and can degrade during processing at high temperatures [16–18]. So, PBSu is most often copolymerized with adipic acid or other monomers, or blended with several different polymers including PLA, cellulose derivatives, poly(caprolactone) (PCL), poly(butylene adipate-co-terephthalate) (PBAT) [16–18]. The European market of PBSu is predicted to grow at a Compound Annual Growth Rate (CAGR) of 14.3% in 2023–2033 [19].

When < 40 wt% of PBSu is added in PLA to give blends, its ductility and melt processability are improved [14, 17]. PLA-co-PBSu copolymers can be used as compatibilizers in these PLA-PBSu blends, resulting in decreased interfacial tension [20–22], or they can be used to prepare PLA-based blends with improved toughness, elongation and crystallization [23–27]. In contrast, blending PBSu in PLA is not very effective in improving its crystallization [26]. The PLA-co-PBSu copolymers reported in the literature were either commercially available (GS Pla® AZ-type with 3 mol% lactate) or synthesized with melt polycondensation which took a total of at least 7 h. In most cases, the main component was PBSu [20, 21, 28, 29]. PLLA-b-PBSu-b-PLLA copolymers have also been reported with small PBSu contents (0.3–35 mol%), synthesized by the traditional routes that lasted 24 h, and were used as compatibilizers in PLA-PBSu blends [22, 27].

Reactive extrusion (REX) is a fast, economically viable method commonly used to functionalize, blend and compatibilize polymers, including PLA, in an industrial setting [11]. Less frequently, REX is used to synthesize PLA by ring opening polymerization (ROP) of lactide [30–33]. When adding a second comonomer in the REX of PLA, such as ε-caprolactone, random copolymers can be obtained [34], while when adding another polymer or oligomer, it acts as a macroinitiator and blocky copolymers are formed [33]. This procedure can also be performed in pilot scale [35].

In our previous work, we synthesized PLA-co-poly(propylene adipate) (PPAd) blocky copolymers in under 20 min via reactive processing, and the PPAd moieties (up to 15 wt%) improved the elongation of PLA and its hydrolytic degradation rates [33, 36, 37]. In contrast, copolymerization with the classical two-stage transesterification and polycondensation method can last up to several hours. In this work, we investigate the synthesis and the properties of fully biobased PLA-PBSu copolymers via reactive processing (to mimic REX in a smaller scale) in a torque rheometer. L-lactide monomer and different amounts of PBSu with two different molecular weights were premixed and fed in the rheometer, using tin(II) 2-ethylhexanoate catalyst, while monitoring the torque. The reactions of all copolymers were completed in under 15 min. The resulting copolymers were characterized in terms of their intrinsic viscosity and molecular weight, chemical structure, thermal and nanomechanical properties.

Materials and Methods

Materials

L-Lactide (LA) Purlact® B3 (purity 99% w/w, stereochemical purity in L-isomer 95% (w/w)) was purchased from Corbion N.V. (Gorinchem, Netherlands), Tin(II) 2-ethylhexanoate $Sn(Oct)_2$, and Titanium(IV) isopropoxide $Ti(OCH(CH_3)_2)$ and all other reagents were of analytical grade and purchased from Merck KGaA, Darmstadt, Germany.

Synthesis of Low Molecular Weight PBSu

PBSu polyesters with different molecular weight were synthesized by two-stage melt polycondensation. In the first stage (esterification), succinic acid and 1,4-butanediol in a 1/1.1 molar ratio were charged into the reaction tube. The reaction mixture was heated at 170 °C–190 °C under nitrogen atmosphere under continuous stirring. The reaction lasted for about 4.5 h, until the theoretical amount of H_2O produced during the reaction was collected. In the second stage (polycondensation), 400 ppm of Titanium(IV) isopropoxide in toluene with respect to the succinic acid was added. The temperature was increased to 240 °C and a vacuum (5.0 Pa) was slowly applied for about 15 min, to minimize the creation of foam and the polycondensation procedure was carried out for 0.5 h resulting in $PBSu_{022}$ with $[\eta] = 0.22$ g/dL or for 1 h producing a $PBSu_{0.38}$ with $[\eta] = 0.38$ g/dL.

Synthesis of PLA-co-PBSu Via Reactive Processing

PLA and its copolymers with PBSu were prepared by reactive processing in a Brabender® Plasti-Corder® Lab-Station torque rheometer with a measuring mixer of 50 cm^3 of capacity. Roller type blades were used, suitable for the

processing of thermoplastics according to the manufacturer. The ROP of lactide was catalysed by $Sn(Oct)_2$ in a lactide/$Sn(Oct)_2$ molar ratio 1000/1. Triphenyl phosphine (TPP) was used as co-catalyst, in equimolar amount to $Sn(Oct)_2$ [38]. The catalyst system was added as a solution in dry toluene. PBSu (diol) was added as initiator for the ROP of lactide to obtain PLA-co-PBSu copolymers. Blank samples without macroinitiator (ROP initiated by traces of H_2O) were also prepared. The polymerization was carried out at 180 °C in the mixer, with a 100 rpm screw speed. A small stream of dry N_2 was circulated to minimize the presence of air in the mixer. The premix of lactide/PBSu/catalyst solution was fed to the mixer of the rheometer at t = 0. Motor torque (which is proportional or related to material's viscosity) and temperature were monitored vs. time during the polymerization. The samples prepared are listed in Table 1.

Physicochemical Characterization

The molecular weight of the materials was determined using gel permeation chromatography (GPC) with a Waters Alliance 2690 pump, Waters Ultrastyragel columns HR-1, HR-2, HR-4E, HR-4 and HR-5, and a Waters Refractive Index Detector 2414. For the calibration, 9 polystyrene (PS) standards of molecular weight between 2.5 and 900 kg/mol were employed. The prepared solutions had a concentration of 10 mg/mL in chloroform, the injection volume was 150 µL, flow rate 1 mL/min and the total elution time was 50 min. The oven temperature was 40 °C.

The intrinsic viscosity of the produced polyesters was measured with an Ubbelohde viscometer (Schott Geräte GMBH, Hofheim, Germany) at 25 °C using chloroform. The sample was heated in the solvent mixture at 80 °C for 20 min until complete dissolution. After cooling, the solution was filtered through a disposable Teflon filter to remove possible solid residues. The calculation of the intrinsic viscosity value of the polymer was performed by applying the Solomon–Ciuta Eq. (1) of a single point measurement [39]:

$$[\eta] = \frac{\left[2\left\{\frac{t}{t_0} - \ln\left(\frac{t}{t_0}\right) - 1\right\}\right]^{1/2}}{c}, \quad (1)$$

where c is the solution concentration, t is the flow time of the solution and t_0 is the flow time of the solvent. The experiment was performed three times and the average value was estimated.

Nuclear Magnetic Resonance (NMR) spectra were recorded in deuterated chloroform. An Agilent 500 spectrometer was utilized (Agilent Technologies, Santa Clara, CA, USA), at room temperature. Spectra were calibrated using the residual solvent peaks.

FTIR-ATR spectra of the samples were recorded utilizing an IRTracer-100 (Shimadzu, Japan) equipped with a QATR™ 10 Single-Reflection ATR Accessory with a Diamond Crystal. The spectra were collected in the range from 450 to 4000 cm^{-1} at a resolution of 2 cm^{-1} (total of 16 co-added scans), while the baseline was corrected in absorbance mode.

Differential Scanning calorimetry (DSC) analysis was performed using a PerkinElmer Pyris Diamond DSC differential scanning calorimeter calibrated with pure indium and zinc standards. The system included a Perkin Intracooler 2 cooling accessory. Samples of 5 ± 0.1 mg sealed in aluminium pans were used to test the thermal behaviour of the polymers after quenching from the melt with a cooling rate of 50 °C/min. The degree of crystallinity was calculated using the following equation:

Table 1 List of the homopolymers and copolymers prepared and their final mol% PBSu content (calculated by NMR)

Abbreviation	Intrinsic viscosity of PBSu (dL/g)	PBSu in the premix (wt%)	PBSu in the premix (mol%)	PBSu calculated by NMR (mol%)[a]
PLA	–	–	–	–
$PLA\text{-}PBSu_{0.22}$ 1	0.22	1	1	1
$PLA\text{-}PBSu_{0.22}$ 2.5	0.22	2.5	2	3
$PLA\text{-}PBSu_{0.22}$ 5	0.22	5	4	6
$PLA\text{-}PBSu_{0.22}$ 10	0.22	10	9	11
$PLA\text{-}PBSu_{0.22}$ 15	0.22	15	13	17
$PLA\text{-}PBSu_{0.38}$ 1	0.38	1	1	1
$PLA\text{-}PBSu_{0.38}$ 2.5	0.38	2.5	2	3
$PLA\text{-}PBSu_{0.38}$ 5	0.38	5	4	6
$PLA\text{-}PBSu_{0.38}$ 10	0.38	10	9	11
$PLA\text{-}PBSu_{0.38}$ 15	0.38	15	13	17

[a]Detailed in "Chemical structure" section

$$Xc(\%) = \frac{\Delta Hm - \Delta Hcc}{\Delta H_m^0 * (1 - \frac{PBSuwt\%}{100})} * 100 \quad (2)$$

where Xc is the % crystallinity, ΔHm is the melting enthalpy, ΔHcc is the cold crystallization enthalpy, and $\Delta H^0{}_m$ is the melting enthalpy of 100% crystalline PLA (93 J/g) [40].

X-Ray Diffraction (XRD) measurements of the polymers and copolymers were performed over the 2θ range of 5 to 60°, with steps of 0.05°, scanning speed 1.5 deg/min, using a MiniFlex II XRD system from Rigaku Co. (Tokyo, Japan) with Cu Ka radiation ($\lambda = 0.154$ nm).

TGA measurements were carried out using a NETZSCH STA 449F5 instrument (NETZSCH Group, Germany), in the temperature range 30 °C–600 °C, heating rate 20 °C/min under nitrogen atmosphere.

The nanoindentation tests were performed using a DUH-211S Shimadzu device (Kyoto, Japan) with a force resolution of 0.196 μN. The tests utilized a diamond triangular tip Berkovich indenter with an angle of 65° and a tip radius of 100 nm. The hardness values were calculated based on the indentation depth and the predetermined applied force. The calculation of the elastic modulus and hardness was based on the Oliver and Pharr method [41] and previous work [41–46]. The maximum applied force was 10 mN and was achieved with a rate of 1.46 mN/s. In order to calculate the nanomechanical properties, five measurements were carried out at different locations for each experiment and the average values were reported. Due to the material's viscoelastic nature, a dwell time of 3 s was implemented to allow sufficient time at peak load for the creep effects to saturate. The additional depth induced during the dwell time at constant load was recorded to provide insight in the creep response of the material. A finite element analysis (FEA) process has been developed in order to fit the nanoindentation test curves and extract the stress–strain behavior of the specimens. The interface between the indenter and the surface of the sample was simulated with contact elements and assumed frictionless. The nanoindentation experiments have been computationally generated considering the simulation of the loading stage of the indenter penetrating the surface. Other works [41–46] have shown that kinematic hardening leads to a rapid convergence in the corresponding FEA calculations, so this method was utilized in the developed curve-fitting procedure.

Results and Discussion

Synthesis of PLA-PBSu Copolymers by Reactive Processing

PLA and its copolymers with PBSu were synthesized with ROP using L-lactide and different molecular weight PBSu as initiators. The temperature of 180 °C for reactive processing was chosen based on previous work, as it gave polymers with higher molecular weight than ROP at 190 °C [33]. The rheograms recorded during the synthesis are shown in Fig. 1, and the molecular weight of the obtained samples are included in Table 1. All GPC chromatographs had unimodal molecular weight distribution (Fig. S1). With the addition of up to 2.5 wt% $PBSu_{0.22}$, the residence time for torque stabilization was 10–20 min, which based on previous experience indicates that it should be compatible with continuous REX, and it has suitable melt strength and viscosity for extrusion grade materials. However, depending on feeding rate, extruder dimensions and rotational speed of a given extruder the time might need to be adjusted so the transferability to an extruder will be tested in the near future. In contrast to

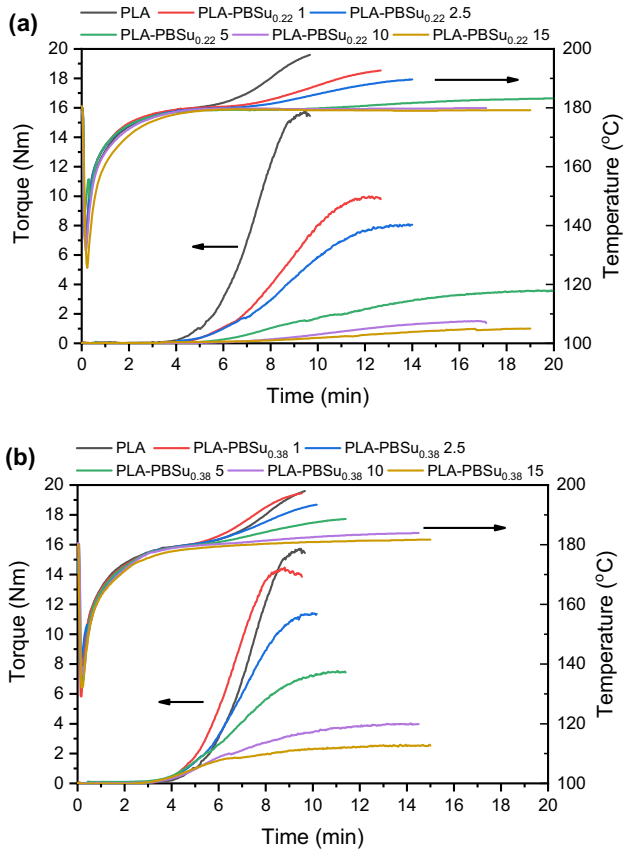

Fig. 1 Torque/temperature curves for ROP of PLA initiated by **a** $PBSu_{0.22}$ and **b** $PBSu_{0.38}$ during reactive processing

the short reaction times required for reactive processing, to prepare such polymers with the conventional melt polycondensation method several hours are needed, under inert atmosphere and high vacuum.

With the addition of 5 wt% $PBSu_{0.22}$ (Fig. 1a), some melt strength is retained yielding the polymer PLA-$PBSu_{0.22}$ 5 suitable for injection moulding grade materials, but high residence time was required. Increasing the content of $PBSu_{0.22}$ further (10 and 15 wt%) led to very low torque values and poor melt strength. On the other hand, good melt strength, viscosity and suitability for continuous reactive processing were retained with adding up to 5 wt% $PBSu_{0.38}$ (Fig. 1b). PLA with 10 wt% $PBSu_{0.38}$ could be used for injection moulding while 15 wt% yielded low torque and melt strength. In both cases, PBSu acted as an initiator, and the polymerization started earlier than for neat PLA, but the maximum torque (viscosity) was lower. The higher the molecular weight of PBSu, the faster the polymerization and higher torque values recorded, thus $PBSu_{0.38}$ was found the better option as an initiator for the reactive processing of PLA.

In line with the reduced torque values, the M_n (Table 2) also decreased with the addition of PBSu. The M_n of neat PLA was 102900 g/mol, which is similar to extrusion grade PLA available in the market. The copolymers with $PBSu_{0.38}$ had higher M_n values in comparison with their homologues with $PBSu_{0.22}$. Overall, there was a decreasing trend of the M_n with increasing PBSu content, except for the polymers PLA-$PBSu_{0.38}$ 1, PLA-$PBSu_{0.38}$ 2.5 and PLA-$PBSu_{0.38}$ 5 which had similar M_n, despite the reduction of their torque. This suggests that besides M_n, other factors can affect torque, such as the low melt viscosity of PBSu. This decreasing trend was also reported for PLA-poly(propylene adipate) copolymers synthesized by reactive processing. As the concentration of hydroxyl groups increases, the ratios of lactide and catalyst to macroinitiator hydroxyls decreases, while the ratio of lactide to catalyst is kept constant. So, the increased number of hydroxyl groups in the reaction that act as initiation sites result in more simultaneously growing PLA chains and fewer active tin alkoxide species, ultimately reducing the molecular weight [33]. The obtained molecular weights might differ from theoretical expectations because of multiple reasons including incomplete conversion and variations in chain length (PDI > 1). Additionally, degradation reactions take place during reactive processing/extrusion attributed to mechanical and oxidative degradation and can result in overprediction of the molecular weight [47].

Despite the decreasing trend of the M_n, when comparing the values with the literature for PLA-PBSu copolymers rich in PBSu prepared by melt polycondensation, either random or block, the maximum M_n achieved was approximately 17000 g/mol and in all cases the reaction time was at least 7 h [20, 21, 28, 29]. It is important to note however that all these copolymers were either equimolar or rich in PBSu. In the literature, to synthesize PLA-b-PBSu-b-PLA with M_n to 16000 g/mol using 1 mol% PBSu of $M_n = 5000$ g/mol, the polycondensation reaction time was 24 h [22]. When PBSu with $M_n = 17000$ g/mol was used, the obtained copolymers with 5 mol% PBSu had $M_n = 83000$ g/mol, but the polycondensation reaction time was again 24 h [27].

Table 2 Molecular weight and PDI of the prepared polymers as measured by GPC

Sample	M_n (g/mol)	M_w (g/mol)	PDI
$PBSu_{0.22}$	6100	13200	2.2
$PBSu_{0.38}$	16300	26000	1.59
PLA	102900	169700	1.65
PLA-$PBSu_{0.22}$ 1	76000	123300	1.62
PLA-$PBSu_{0.22}$ 2.5	79600	121100	1.52
PLA-$PBSu_{0.22}$ 5	49700	77800	1.56
PLA-$PBSu_{0.22}$ 10	31000	49400	1.59
PLA-$PBSu_{0.22}$ 15	31900	46700	1.46
PLA-$PBSu_{0.38}$ 1	77400	122800	1.58
PLA-$PBSu_{0.38}$ 2.5	79000	124300	1.57
PLA-$PBSu_{0.38}$ 5	80200	125400	1.56
PLA-$PBSu_{0.38}$ 10	54200	78900	1.45
PLA-$PBSu_{0.38}$ 15	39000	55400	1.42

Chemical Structure

The chemical structure of the produced copolymers was examined with NMR and FTIR-ATR spectra. The ^{1}H-NMR and ^{13}C-NMR spectra are presented in Fig. 2.

First, PBSu was synthesized by the melt polycondensation of succinic acid and excess 1,4-butanediol. Because of the excess diol, the synthesized PBSu is expected to be hydroxyl-terminated. The ^{1}H spectra of $PBSu_{0.22}$ and $PBSu_{0.38}$ (Fig. 2a and b) have strong resonance signals that are explained below, but also weak resonance signals at 3.67 ppm (Fig. S2) that are assigned to the methylene proton of $–CH_2OH$ and reveal the presence of hydroxyl-terminated chains [48]. No signal that could be associated with terminal $–CH_2COOH$ groups is detected in the region around 2.5 ppm, further supporting that the PBSu has terminal hydroxyl groups [49].

Both ^{1}H and ^{13}C spectra confirm the successful polymerization of L-lactide in the presence of $PBSu_{0.22}$ and $PBSu_{0.38}$ to afford the corresponding copolymers. Notably, in the ^{13}C spectra (Fig. 2c and d), we can observe the resonance signals corresponding to the C=O of the esters of the PLA and PBSu segments at 169.5 and 172.2 ppm, respectively. Furthermore, the $–CH_2OH$ end chain moieties that can be detected in the ^{1}H spectra of the two PBSu homopolymers at 3.67 ppm are not observable anymore in

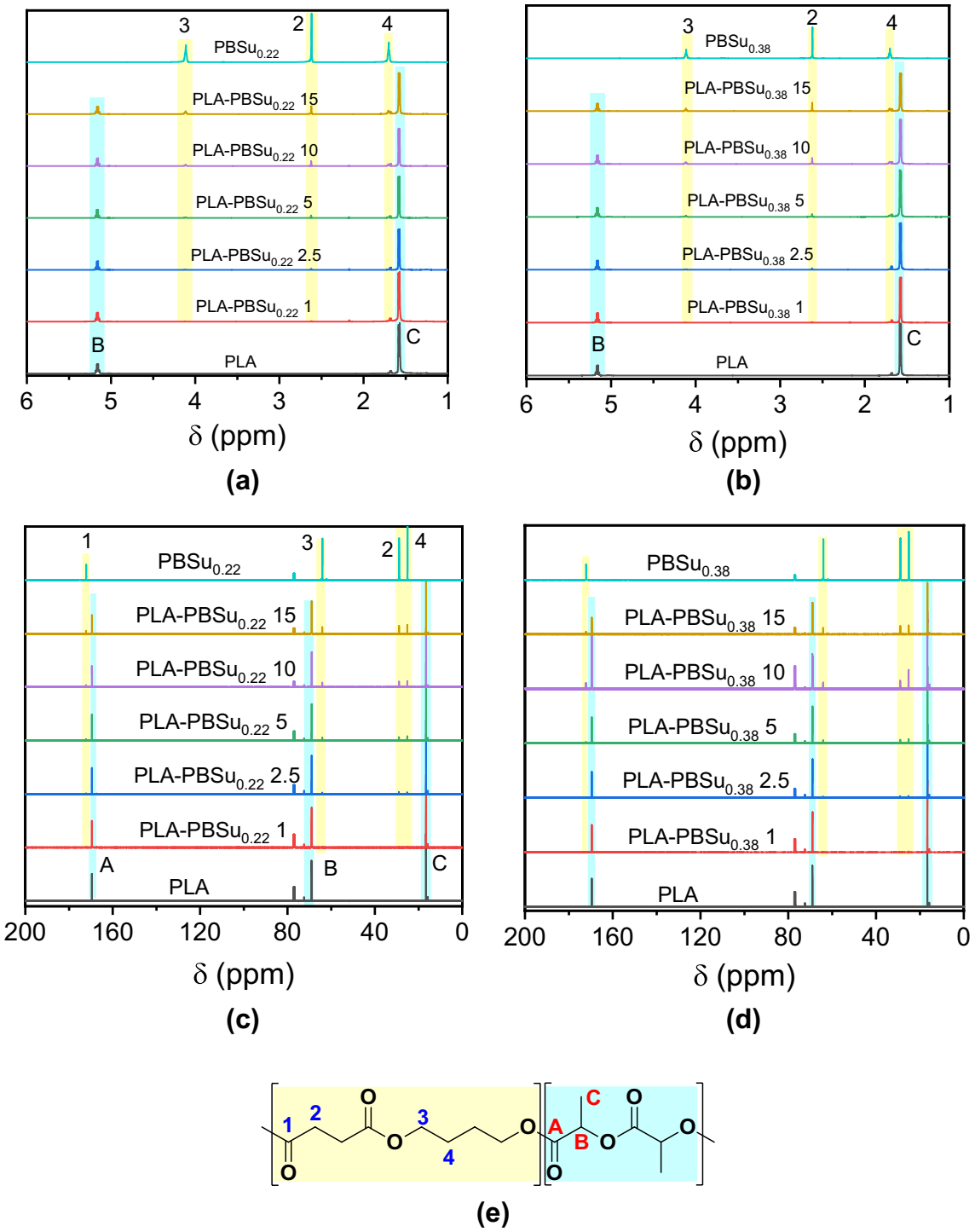

Fig. 2 **a**, **b** ^{1}H NMR and **c**, **d** ^{13}C NMR spectra of the synthesized copolymers and the corresponding homopolymers, **e** signal assignments. Left: polymers with $PBSu_{0.22}$; right: polymers with $PBSu_{0.38}$

the spectra of the copolymers indicating that PBSu, acting as a macroinitiator, reacts through its end-groups to initiate the ROP of L-lactide. Traces of unreacted LA can be seen around 5 ppm. Otherwise typical resonance signals of PLA and PBSu units are observed: 1.58 ppm ($-CH_3$ **C**, PLA), 1.70 ppm ($-CH_2-$ **4**, PBSu), 2.62 ppm ($C(O)CH_2-$ **2**, PBSu), 4.11 ppm ($-OCH_2-$ **3**, PBSu), and 5.16 ppm (CH **B**, PLA) for the ^{1}H spectra; 16.6 ppm ($-CH_3$ **C**, PLA), 25.2 ppm ($-CH_2-$ **4**, PBSu), 29.0 ppm ($C(O)CH_2-$ **2**, PBSu), 64.1 ppm ($-OCH_2-$ **3**, PBSu), 68.9 ppm (CH **B**, PLA), 169.5 ppm

(C = O **A**, PLA) and 172.2 ppm (C=O **1**, PBSu) for the ^{13}C spectra (Fig. 2c and d). Finally, the composition of the copolymers was estimated by comparing the integrations of the PLA CH (5.16 ppm) and PBSu OCH_2 (4.11 ppm) resonance signals. A good agreement with the feed ratio was found, as shown in Table 1 and Table S1. The excess of PBSu found in the final copolymers could be due to the small amounts of unreacted L-lactide or to some monomer sublimation during the extrusion process. Unfortunately, as both PLA and PBSu are aliphatic polymers and due to the relatively small amounts of PBSu incorporated in the copolymers, it is not possible to differentiate the signals corresponding to the protons of the PBSu units connected to PLA units (PBSu-$OCH_2CH_2CH_2CH_2$-C(O)CH(CH_3)-O-PLA) and further discuss the microstructure of the copolymers (*i.e.* random or block copolymers, and block length). Nevertheless, according to previous work, PLA-b-PBSu-b-PLA triblocky or PLA-b-PBSu diblocky copolymers are expected in the case that PBSu has two -OH end groups or one -OH groups, respectively [22, 27, 33]. Because of the difficulty to prove the presence of only block copolymers, we must keep in mind that it is possible that a blend composition was received, comprised of PLA homopolymer and PLA-b-PBSu-b-PLA copolymer. Thus, the copolymers received are referred to as blocky.

In Fig. S3, the FTIR-ATR spectra of PLA, PBSu and their copolymers are presented. The spectrum of PLA showed absorption bands at 2900–3000 cm^{-1} of C–H stretching, at 1746 cm^{-1} caused by the C=O stretching of polyesters, at 1452 cm^{-1} of $–CH_3$ bending, and C–O–C stretching at 1180 cm^{-1} and 1081 cm^{-1}. PBSu had its main absorption bands at 2945 cm^{-1} assigned to C–H stretching vibrations of the CH_2 groups, at 1713 cm^{-1} caused by the stretch vibrations of C=O, at 1472 cm^{-1} due to CH_2 bending, at 1425 cm^{-1} due to CH_2 stretching, at 1330 cm^{-1} due to C–H stretching vibrations, at 1153 cm^{-1} from C–O–C stretching, and at 1044 cm^{-1} due to C–H bending of the CH–OH group [50, 51]. Upon closer examination of the region 1800–1200 cm^{-1} (Fig. 3), the evolution of PBSu-related absorption bands in the spectra of the copolymers can be seen in the copolymers with the higher PBSu content. More specifically, the C=O bands of both PLA and PBSu appeared, and the bands caused by vibrations of the groups of PBSu, namely CH_2, appeared in the spectra of PLA-PBSu 10 and 15 wt%.

Thermal Transitions and Crystallinity

The thermal transitions of the synthesized polymers were studied with DSC. The curves obtained by heating the samples with a rate of 20 °C/min after quenching are presented in Fig. 4. PLA has a $T_g = 55.6$ °C, $T_{cc} = 115.2$ °C and a double melting point at $T_{m1} = 166.8$ °C and $T_{m2} = 172.2$ °C caused by crystal reorganization during heating. PBSu is

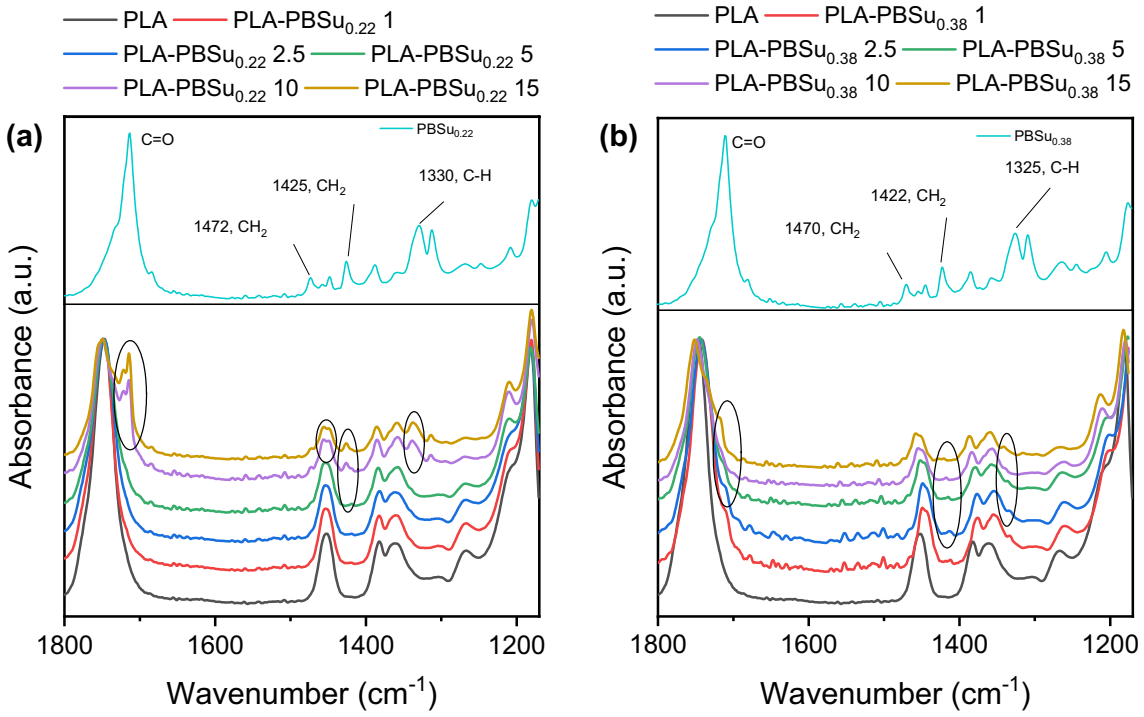

Fig. 3 FTIR-ATR spectra of **a** PLA-$PBSu_{0.22}$ copolymers and **b** PLA-$PBSu_{0.38}$ copolymers in the region 1800–1200 cm^{-1} and peak assignments of PBSu (light blue spectra). The copolymer spectra are normalized to the PLA C=O band at ~ 1745 cm^{-1} (Color figure online)

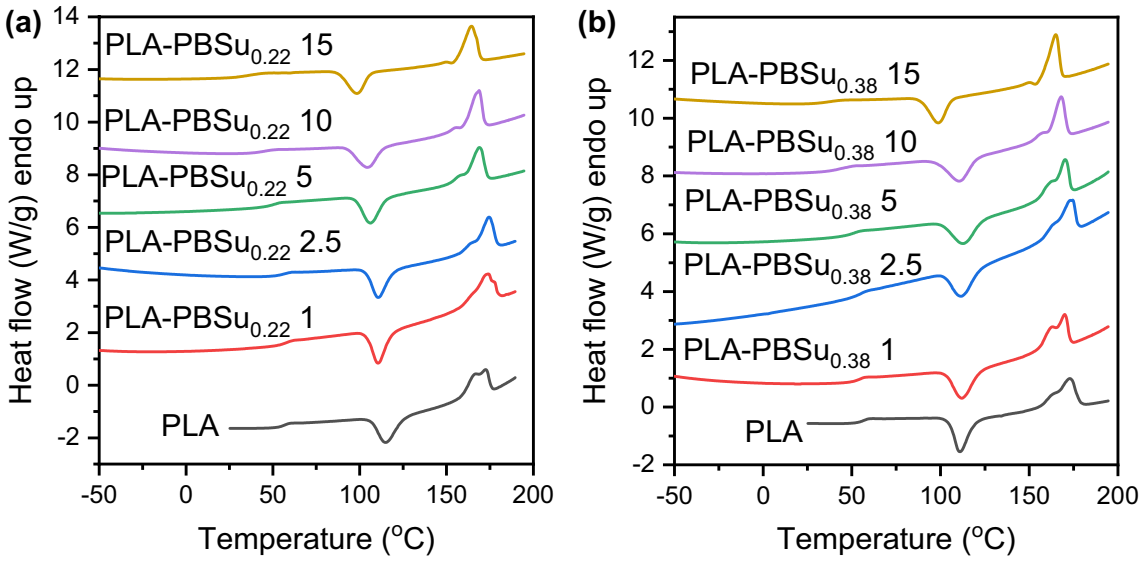

Fig. 4 DSC heating scans of **a** PLA-$PBSu_{0.22}$ copolymers and **b** PLA-$PBSu_{0.38}$ copolymers after quenching with heating rate 20 °C/min

a fast crystallizing polyester that exhibits multiple melting behaviour due to melt-recrystallization and has a ΔH_m^0 =210 J/g [52]. From the DSC scans of Fig. S4 a the recrystallization and subsequent melting are observed at 95.8 °C and 108.1 °C for $PBSu_{0.22}$ and at 97.9 °C and 105 °C for $PBSu_{0.38}$. The ultimate peak of the final melting is recorded at 113.8 °C and 114.5 °C for $PBSu_{0.22}$ and $PBSu_{0.38}$, respectively. The slight increase of the recrystallization and melting peak temperatures are attributed to the larger molecular weight of $PBSu_{0.38}$ and therefore longer and more rigid chains with stronger intermolecular interactions that require more thermal energy to overcome.

The DSC heating scans of the PLA-PBSu copolymers are similar to the one of PLA (Fig. 4), with small shifts of the peaks. During cooling from the melt it was observed that none of the copolymers contained the sharp melt crystallization peak of PBSu, (Figure S5) which occurs at around 80 °C–85 °C [53]. The effect of the introduction of the PBSu moieties in PLA on its thermal characteristics is shown in Fig. 5. A single T_g is detected in all copolymers, which was the case for triblock PLA-PBSu-PLA copolymer with PBSu content 27–90 mol%, attributed to a miscible amorphous phase [54]. In both PLA-co-PBSu copolymers series, T_g, T_{cc} and T_m have a decreasing trend, which agrees with the decreasing M_n trend (Table 2). Since the T_g decreases also in similar M_n copolymers with the increase of the PBSu content (i.e. PLA-$PBSu_{0.38}$ 1, PLA-$PBSu_{0.38}$ 2.5 and PLA-$PBSu_{0.38}$ 5), it can be assumed that both the reduced chain length and the presence of PBSu play a role in softening due to the modified micro/nanostructure of the continuous phase by PBSu. The decrease of T_{cc}, and therefore the improvement of crystallizability is more pronounced in the

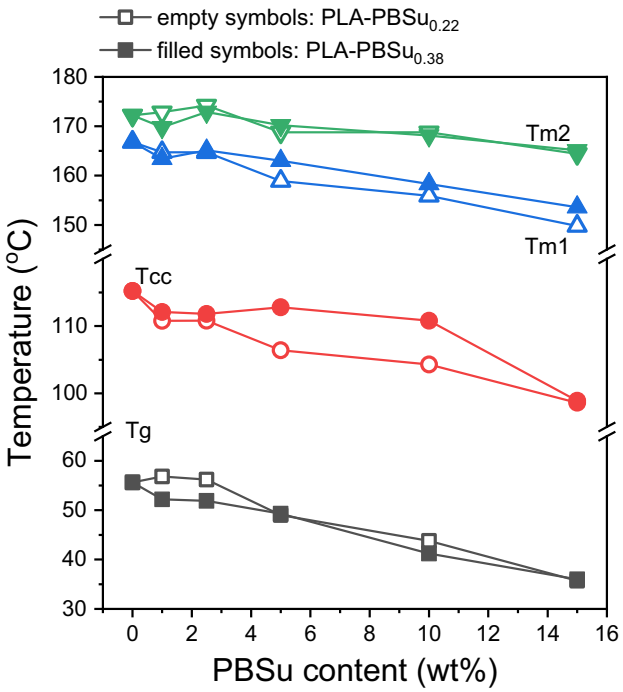

Fig. 5 Effect of the molecular weight and concentration of PBSu on the thermal characteristics of PLA (heating rate 20 °C/min). The lines are used to guide the eyes

copolymers PLA-$PBSu_{0.22}$ since they have lower M_n and their chains can fold into lamellae more easily. Because the T_m of PBSu occurs in the same temperature range as the T_{cc} of PLA during heating with 20 °C/min, scans were also recorded at 10 °C/min to see if melting of PBSu can be detected. Only one copolymer, PLA-$PBSu_{0.22}$ 15 had a weak

melting peak at around 100 °C (Figure S6) when heating with 4 °C/min, which can be associated with PBSu moieties that crystallized. The crystallization of the copolymers will be studied in more depth in a future paper.

The XRD patterns of PLA and its copolymers with different molecular weight PBSu, recorded after isothermal cold crystallization are presented in Fig. 6. Both PLA and PBSu are semicrystalline materials with strong diffraction peaks. The PLA homopolymer had diffraction peaks at 2θ = 14.7° (010), 16.4° (200/110), 18.7° (203), and 22° (210), while PBSu had peaks at 19.6° (020), 21.9° (021), 22.6° (110) and 28.7° (111) [17]. All copolymers had the diffraction peaks of PLA, but it is difficult to conclude if the peaks after 20° are a result of diffractions of PBSu crystals because of overlap with the peaks of PLA. It is however worth noting that a weak diffraction peak that matches the position of the peak of PBSu at 28.7° seems to appear in the copolymers with PBSu content > 5%. In combination with the identification of melting of PBSu moieties in the copolymer PLA-$PBSu_{0.22}$ 15 (Figure S6), there are indications that PBSu crystals might form simultaneously with PLA crystals for high PBSu content of low molecular weight. When the PLA block length was larger than 7.8 repeating units, it was reported that both PLA and PBSu crystals coexisted [54].

Thermal Stability

The thermal stability of PLA and its copolymers with PBSu was examined using TGA. The recorded mass loss and DTG graphs are shown in Fig. 7 and the thermal degradation characteristics are presented in Table S2. PLA is thermally stable until 270 °C, where its degradation starts and is completed in one step at 315 °C. PBSu, regardless of its molecular weight is more thermally stable than PLA [54], as its degradation does not start until ~ 350 °C (Fig. S7), which can be attributed to its longer aliphatic segment. All PLA-PBSu copolymers exhibit two distinct degradation steps, the first corresponding to their PLA segments and the second to their PBSu segments. The copolymers with 1 wt% PBSu in the feed (PLA-$PBSu_{0.22}$ 1 and PLA-$PBSu_{0.38}$ 1, red lines in Fig. 7) are an exception, as the PBSu content wasn't high enough to detect a separate degradation step. The $T_{o,1}$ and $T_{p,1}$ of the PLA segments are not significantly affected by the presence of PBSu in general. In contrast, the $T_{o,2}$ and $T_{p,2}$ of the PBSu segments are lower than these of neat PBSu. In the DTG graphs (Fig. 7b and d), the shifting of the peaks shows that by increasing the amount of PBSu in the copolymers, the thermal stability of the PLA segment decreased, and the thermal stability of the PBSu segments increased. The thermal stability of PLA blocks has been reported to increase as their block lengths increased and vice versa, so as the PLA content and molecular weight of the copolymers decreases, the PLA block length is smaller, and more end groups are present in the macromolecular chain [54] Tthe decreased thermal stability of the PLA blocks as the PLA content in the copolymer increases can be due to backbiting or transesterification during heating that might produce vaporizable short chains.

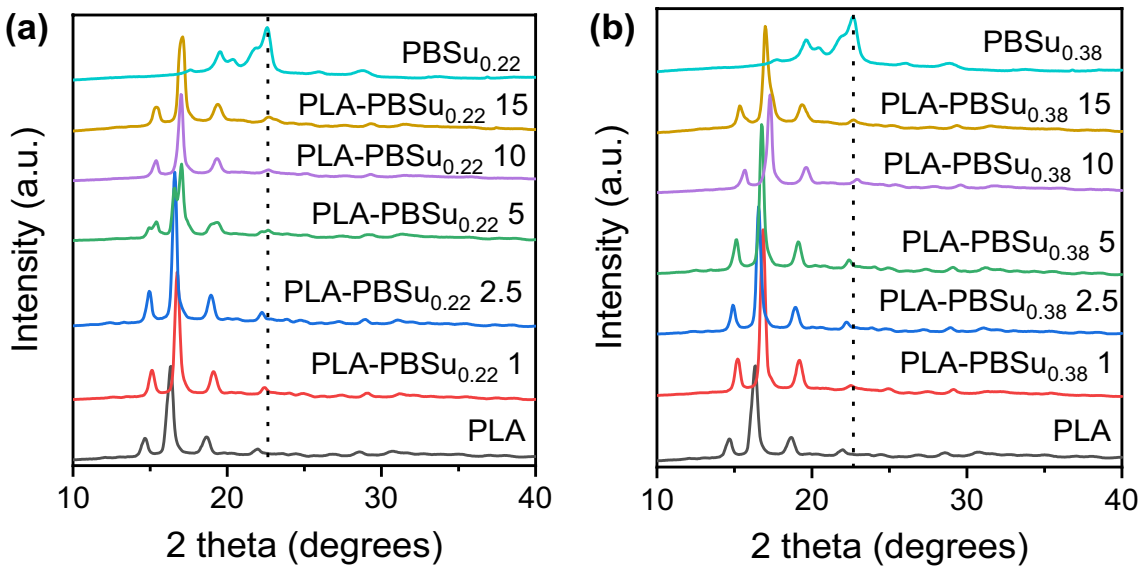

Fig. 6 XRD patterns of **a** PLA and its copolymers with $PBSu_{0.22}$ and **b** PLA and its copolymers with $PBSu_{0.38}$ after isothermal cold crystallization at the T_{cc} peak for 1 h

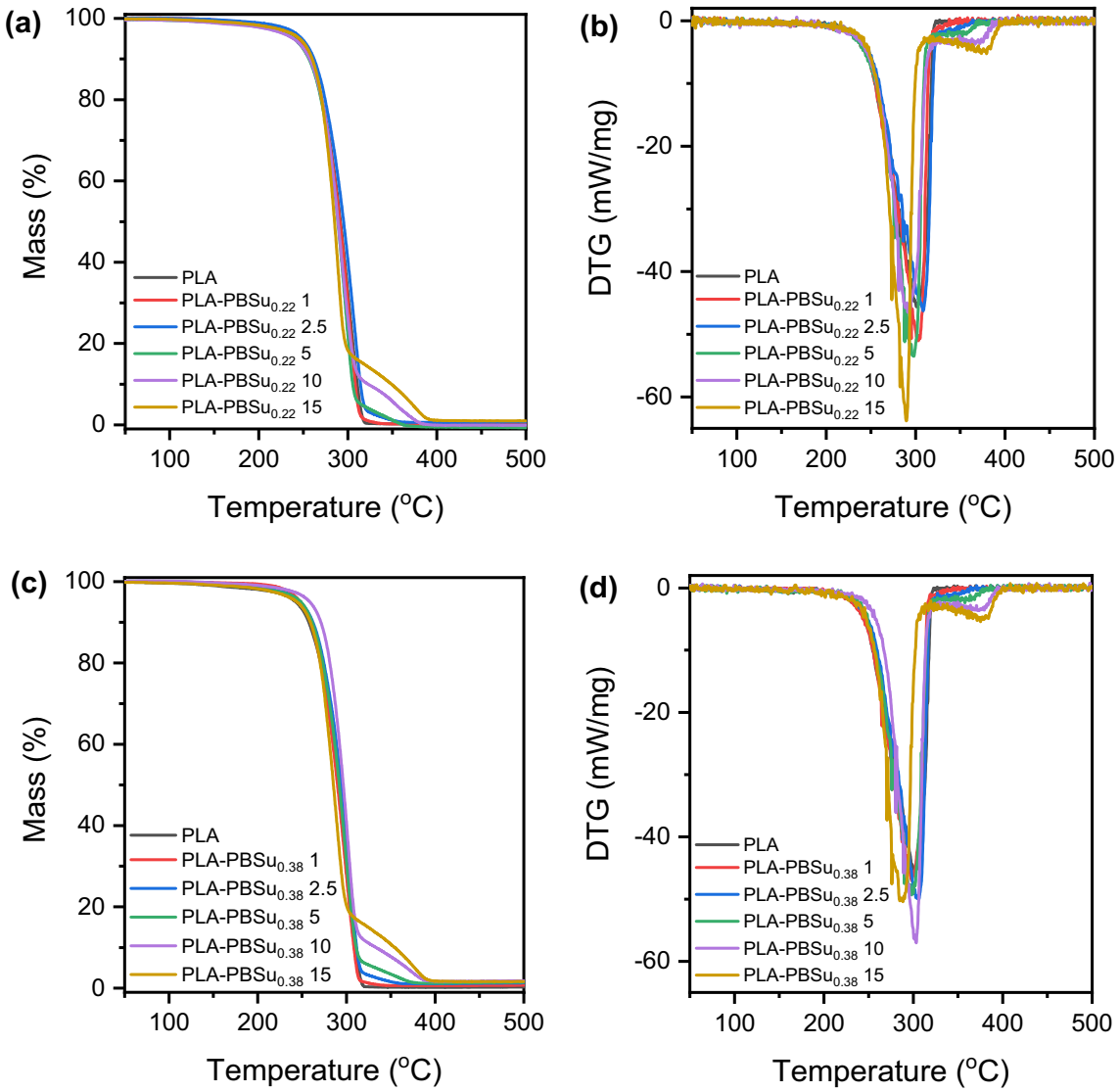

Fig. 7 Mass-temperature and their derivative curves derived from TGA of **a**, **b** PLA and its copolymers with $PBSu_{0.22}$ and **c**, **d** PLA and its copolymers with $PBSu_{0.38}$

Nanomechanical Properties

The mechanical behaviour of PLA-PBSu copolymers was evaluated by nanoindentation testing. The resulting nanoindentation depth curves are presented in Fig. S8. Composition, crystallinity, and molecular weight are the main the properties that affect the mechanical properties of polymers. The specimens used for nanoindentation were prepared with compression moulding using the same conditions, i.e., melting at $T_m + 40$ °C and then the specimens were left to cool at room temperature. The crystallinity of PLA in the as-received specimens from compression molding was estimated by DSC, using a heating rate of 20 °C/min. Because of the different composition and molecular weight of the copolymers however, crystallinity and T_g are not identical between the different polymers but show an increasing trend with the decrease of molecular weight and increase of PBSu content. It is worth noting that the T_g of the compression molded specimens differs from the melt-quenched ones (*MERGEFORMAT Fig. 4 and*MERGEFORMAT Fig. 5) because of the difference in their thermal history. The semicrystalline compression molded specimens had higher T_g values than these melt-quenched (amorphous) in the DSC furnace, as expected (Table 3).

The hardness values of PLA and the copolymers are shown in Fig. 8a. Overall, hardness decreased from 156 ± 36 MPa for PLA down to 57 ± 10 MPa for the copolymer PLA-$PBSu_{0.38}$ 15. The decreasing trend is in line with the M_n reduction (Table 2) and the plasticization concluded from the decrease of the T_g (Fig. 5) and there is no

Table 3 Crystallinity and T_g values calculated by DSC curves of the as-received specimens used for nanomechanical properties that were prepared with compression molding

Sample	T_g (°C)	Crystallinity (%)
PLA	52.2	20.6
PLA-PBSu$_{0.22}$ 1	51.3	18.5
PLA-PBSu$_{0.22}$ 2.5	53.5	25.2
PLA-PBSu$_{0.22}$ 5	52.3	19.2
PLA-PBSu$_{0.22}$ 10	49.7	25.1
PLA-PBSu$_{0.22}$ 15	56.1	30.4
PLA-PBSu$_{0.38}$ 1	53.1	26.1
PLA-PBSu$_{0.38}$ 2.5	52.6	24.7
PLA-PBSu$_{0.38}$ 5	49.1	30.6
PLA-PBSu$_{0.38}$ 10	55.3	29.9
PLA-PBSu$_{0.38}$ 15	53.5	36.7

significant difference in the hardness values between the two series of polymers. An obvious exception in this trend is both copolymers with 2.5 wt% PBSu, which despite their quite different M_n have similar hardness values, both larger than this of PLA. The relatively high M_n in combination with the crystallinity might have synergistically caused the increase of hardness. Elastic modulus (Fig. 8b) increased with 2.5 and 5 wt% PBSu and decreased for all other PBSu contents. In these two compositions, it seems that the effect of crystallinity prevails that of plasticization and causes an increase of the elastic modulus. The trend is similar to that of hardness, with the copolymers containing 2.5% PBSu exhibiting the largest hardness and modulus values. However, with higher concentrations of 10% and 15% PBSu, the hardness and elastic modulus decrease again due to the sharp molecular weight drop. Overall, there are no big differences in the hardness and elastic modulus values between the two copolymer series, i.e. PLA-PBSu$_{0.22}$ and PLA-PBSu$_{0.38}$, except for the copolymers with 5% PBSu which can be attributed to the quite different molecular weights (49700 g/mol vs 80200 g/mol). Deviations of the hardness from the law of additivity has been reported before for block copolymers and have been attributed to either microphase separation or differences in the micromechanical deformation behaviour on the nanometer scale [55]. The decreasing trend of the elastic modulus and stress at break was reported before for PLA-PBSu block copolymers with PBSu contents 5–35 mol%. The elongation of PLA was improved when 25 mol% or 35 mol% of PBSu was incorporated [27].

To conduct FE analysis, the model was introduced with an initial value for the first tangent modulus of the sample's stress–strain curve, which is related to the elastic modulus derived from the nanoindentation tests. The FE model was then subjected to an incremental application of the measured indentation depth on the indenter and the corresponding force reaction was computed and compared to the measured value. The goal was to obtain FEA force-depth data that fits the experimental nanoindentation curve; otherwise, the tangent modulus value had to be recalculated. If the computational force matched the measured force, the value of the tangent modulus was accepted, and the next force and depth values were applied to the model. The subsequent calculation steps considered the previous indentation depth value, the existing stress status, and the previously obtained

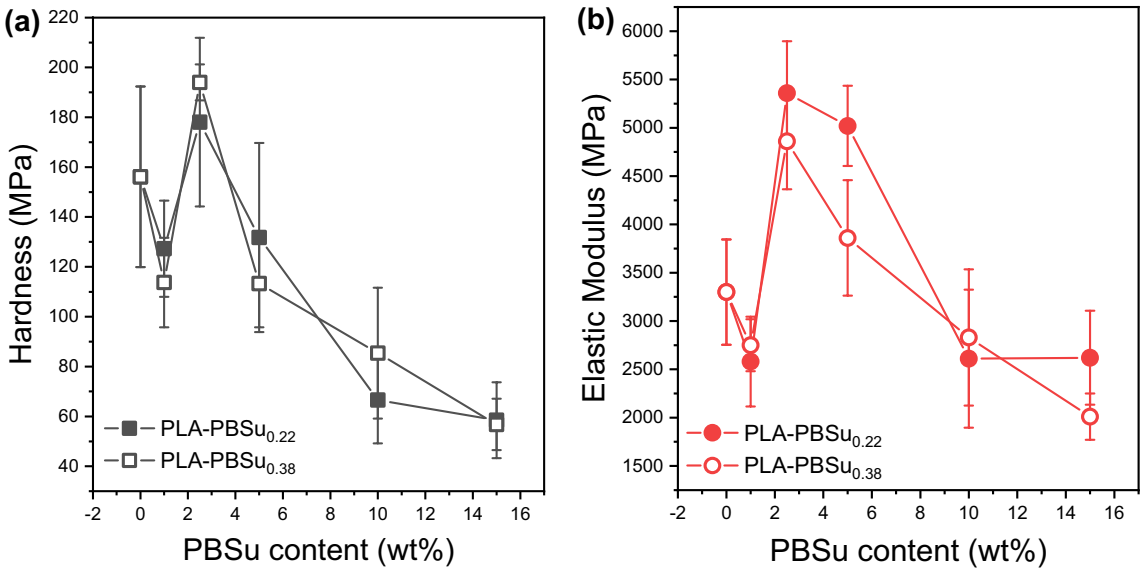

Fig. 8 Effect of PBSu molecular weight and content on **a** Hardness and **b** elastic modulus of the PLA-PBSu copolymers. The lines are used to guide the eyes

tangent modulus. This iterative process continued until the last load-depth values converged and the loop ended. To achieve a satisfactory curve fitting of the nanoindentation curves, at least 20 simulation steps were performed to obtain converged FEA solutions. This methodology allows for the estimation of the materials' constitutive laws by calculating stress–strain curves of polymers based on nanoindentation force-depth data under different testing conditions.

The FEA generated stress–strain curves for PLA and its copolymers with $PBSu_{0.22}$ and $PBSu_{0.38}$ are presented in Fig. 9a and b, respectively. Table 4 shows the convergence between FEA and the experimental elastic modulus values for all the copolymers. The results show a good correlation between the measured nanoindentation tests and the computational data for all specimens. For PLA-PBSu specimens the FE results seem to underpredict the elastic modulus in some cases. This is due to the inherent nature of calculation from the Oliver-Pharr approach, which measures the elastic modulus from the unloading section of the load-depth curve, while the FEA calculates the response from the loading curve up to maximum force. Overall, FEA verifies the nanoindentation results for the increase of modulus for 2.5 and 5%, while only the 2.5% copolymers seem to have higher modulus as compared to the rest of PLA/PBSu specimens. Therefore, PLA-PBSu 2.5 copolymers revealed simultaneously higher elasticity modulus and strength compared to the other copolymers. Considering these results, it can be concluded that the addition of PBSu affected the overall stress–strain behaviour of the 1%,10%,15% copolymers by reducing the elastic modulus values, however from the stress–strain curves the ultimate strains were increased due to flexible macromolecular change of PBSu, confirming the plasticization effect detected by the decrease of T_g. Finally, the experimental nanoindentation technique assisted by FEA has proven to be a very successful method for determining the nanomechanical behaviour of PLA and PLA-PBSu copolymers.

Table 4 Elastic moduli of the PLA-PBSu copolymers determined from nanoindentation and FE analysis

Sample	Elastic modulus (MPa) nanoindentation	Elastic modulus (MPa) FEA
PLA	3300	3353
PLA-$PBSu_{0.22}$ 1	2580	2515
PLA-$PBSu_{0.22}$ 2.5	5360	5123
PLA-$PBSu_{0.22}$ 5	5020	4838
PLA-$PBSu_{0.22}$ 10	2610	1956
PLA-$PBSu_{0.22}$ 15	2620	1467
PLA-$PBSu_{0.38}$ 1	2750	2567
PLA-$PBSu_{0.38}$ 2.5	4860	4694
PLA-$PBSu_{0.38}$ 5	3860	3667
PLA-$PBSu_{0.38}$ 10	2830	2439
PLA-$PBSu_{0.38}$ 15	2010	2090

Conclusions

PLA-PBSu blocky copolymers were successfully prepared with reactive processing with reaction times ≤ 20 min. The number average molecular weights were in the range of 31900–80200 g/mol, it could be regulated by varying the ratio of L-lactide monomer to PBSu in the premix. The

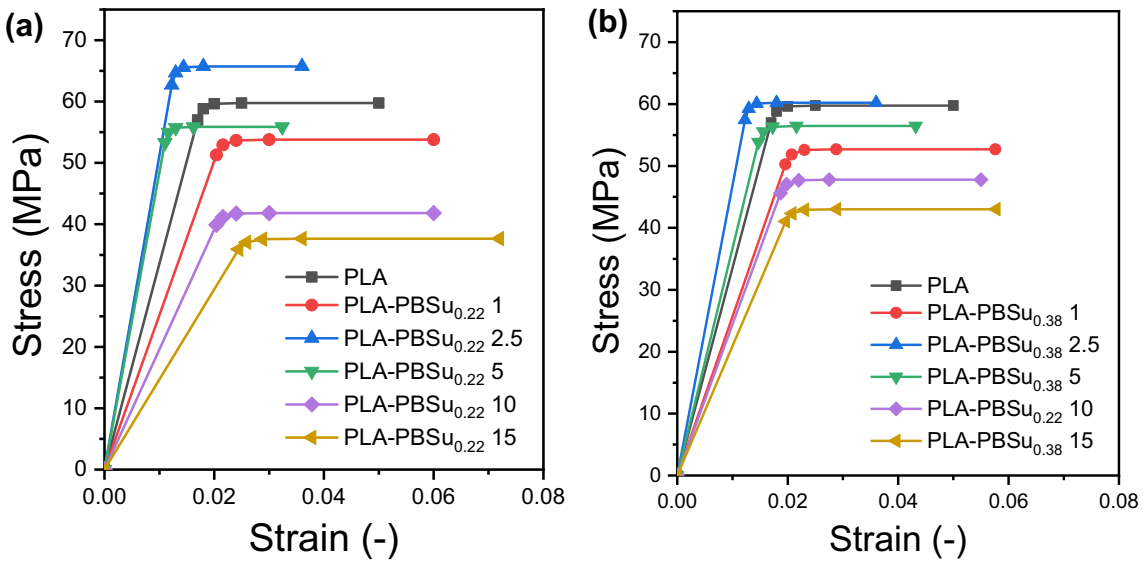

Fig. 9 FEA generated stress–strain curves of **a** PLA and its copolymers with $PBSu_{0.22}$ and **b** PLA and its copolymers with $PBSu_{0.38}$

PLA-based copolymers were found promising for continuous REX for PBSu with [η] = 0.22 dL/g content up to 2.5 wt%, and with PBSu with [η] = 0.38 dL/g content up to 5 wt%. Using higher molecular weight of PBSu ([η] = 0.38 dL/g) resulted in faster polymerization and higher torque values, thus $PBSu_{0.38}$ was deemed a more suitable initiator for the reactive processing of PLA. The copolymerization decreased the T_g and T_m of PLA because of the flexible PBSu segments, and XRD peaks related to cold crystallization emerged from the crystals of PLA and likely PBSu moieties in PBSu contents > 5%. Thermal degradation occurred in two steps and the thermal stability decreased when the M_n was smaller. Future studies are planned to investigate the crystallization and molecular mobility and the effect of the PLA-PBSu copolymers as compatibilizers in PLA-PBSu blends.

Supplementary Information The online version contains supplementary material available at https://doi.org/10.1007/s10924-023-02981-0.

Acknowledgements The authors would like to express their gratitude to Maria Kasimatis from the Department of Chemistry, University of Athens, for performing the GPC measurements.

Author Contributions ZT: investigation, writing—original draft, writing—review & editing, visualization, project administration, supervisionAZ: investigation, writing—original draft, writing—review & editingNDB, AM, AM, SK: investigationMAV: conceptualization, investigation, writing—original draft, writing—review & editing, resourcesKT: formal analysis, writing—original draftDT: resources, writing—original draftKT: writing—original draft, resouces, funding acquisition.

Funding Open access funding provided by HEAL-Link Greece. This work was funded from the European Union's Horizon 2020 Research and Innovation Programme under Grant Agreement No. 952941 (BIOMAC Project).

Data Availability All data are included in the manuscript and supplementary information.

Declarations

Conflict of interest The authors declare no conflicts of interest.

References

1. European Comission Biobased, Biodegradable and Compostable Plastics: https://environment.ec.europa.eu/topics/plastics/biobased-biodegradable-and-compostable-plastics_en. Accessed Jan 27 2023
2. European comission european green deal: putting an end to wasteful packaging, boosting reuse and recycling: https://ec.europa.eu/commission/presscorner/detail/en/ip_22_7155. Accessed Jan 27 2023
3. Farah S, Anderson DG, Langer R (2016) Physical and mechanical properties of PLA, and their functions in widespread applications—a comprehensive review. Adv Drug Deliv Rev 107:367–392. https://doi.org/10.1016/j.addr.2016.06.012
4. DeStefano V, Khan S, Tabada A (2020) Applications of PLA in modern medicine. Eng Regen 1:76–87. https://doi.org/10.1016/j.engreg.2020.08.002
5. Domenek S, Ducruet V (2016) Characteristics and Applications of PLA. Biodegrad Biobased Polym Environ Biomed Appl. https://doi.org/10.1002/9781119117360.ch6
6. Balla E, Daniilidis V, Karlioti G, Kalamas T, Stefanidou M, Bikiaris ND, Vlachopoulos A, Koumentakou I, Bikiaris DN (2021) Poly(lactic acid): a versatile biobased polymer for the future with multifunctional properties-from monomer synthesis, polymerization techniques and molecular weight increase to PLA applications. Polymers (Basel) 13:1822. https://doi.org/10.3390/polym13111822
7. Bikiaris ND, Koumentakou I, Samiotaki C, Meimaroglou D, Varytimidou D, Karatza A, Kalantzis Z, Roussou M, Bikiaris RD, Papageorgiou GZ (2023) Recent Advances in the investigation of poly (lactic acid)(PLA) nanocomposites: incorporation of various nanofillers and their properties and applications. Polymers (Basel) 15:1196
8. Vlachopoulos A, Karlioti G, Balla E, Daniilidis V, Kalamas T, Stefanidou M, Bikiaris ND, Christodoulou E, Koumentakou I, Karavas E (2022) Poly (lactic acid)-based microparticles for drug delivery applications: an overview of recent advances. Pharmaceutics 14:359
9. Nofar M, Sacligil D, Carreau PJ, Kamal MR, Heuzey M-C (2019) Poly (lactic acid) blends: processing, properties and applications. Int J Biol Macromol 125:307–360
10. Kost B, Basko M, Bednarek M, Socka M, Kopka B, Łapienis G, Biela T, Kubisa P, Brzeziński M (2022) The influence of the functional end groups on the properties of polylactide-based materials. Prog Polym Sci 130:101556. https://doi.org/10.1016/j.progpolymsci.2022.101556
11. Augé M-O, Roncucci D, Bourbigot S, Bonnet F, Gaan S, Fontaine G (2023) Recent advances on reactive extrusion of poly(lactic acid). Eur Polym J 184:111727. https://doi.org/10.1016/j.eurpolymj.2022.111727
12. Ali W, Ali H, Gillani S, Zinck P, Souissi S (2023) Polylactic acid synthesis biodegradability, conversion to microplastics and toxicity: a review. Environ Chem Lett. https://doi.org/10.1007/s10311-023-01564-8
13. Stefaniak K, Masek A (2021) Green copolymers based on poly (lactic acid)—short review. Materials (Basel) 14:5254
14. Hamad K, Kaseem M, Ayyoob M, Joo J, Deri F (2018) Polylactic acid blends: the future of green. Light and Tough Prog Polym Sci 85:83–127. https://doi.org/10.1016/j.progpolymsci.2018.07.001
15. Rasal RM, Janorkar AV, Hirt DE (2010) Poly(lactic acid) modifications. Prog Polym Sci 35:338–356. https://doi.org/10.1016/j.progpolymsci.2009.12.003
16. Aliotta L, Seggiani M, Lazzeri A, Gigante V, Cinelli P (2022) A brief review of poly (butylene succinate)(PBS) and Its main

copolymers: synthesis, blends, composites, biodegradability, and applications. Polymers (Basel) 14:844
17. Barletta M, Aversa C, Ayyoob M, Gisario A, Hamad K, Mehrpouya M, Vahabi H (2022) Poly(butylene succinate) (PBS): materials, processing, and industrial applications. Prog Polym Sci 132:101579. https://doi.org/10.1016/j.progpolymsci.2022.101579
18. Savitha KS, Paghadar BR, Kumar MS, Jagadish RL (2022) Polybutylene Succinate, a potential bio-degradable polymer: synthesis. Copolymer Bio-Degrad Polym Chem 13:3562–3612
19. Future Market Insights Polybutylene Succinate Market to Expand at a 14.9% Value CAGR by 2033 | Future Market Insights, Inc. https://www.globenewswire.com/news-release/2023/01/11/2587224/0/en/Polybutylene-Succinate-Market-to-Expand-at-a-14-9-value-CAGR-by-2033-Future-Market-Insights-Inc.html. Accessed Jan 28 2023
20. Supthanyakul R, Kaabbuathong N, Chirachanchai S (2016) Random poly(butylene succinate-Co-lactic acid) as a multi-functional additive for miscibility, toughness, and clarity of PLA/PBS blends. Polymer (Guildf) 105:1–9. https://doi.org/10.1016/j.polymer.2016.10.006
21. Zhang W, Xu Y, Wang P, Hong J, Liu J, Ji J, Chu PK (2018) Copolymer P(BS-Co-LA) enhanced compatibility of PBS/PLA composite. J Polym Environ 26:3060–3068. https://doi.org/10.1007/s10924-018-1180-0
22. Supthanyakul R, Kaabbuathong N, Chirachanchai S (2017) Poly(L-lactide-b-butylene succinate-b-L-lactide) triblock copolymer: a multi-functional additive for PLA/PBS blend with a key performance on film clarity. Polym Degrad Stab 142:160–168. https://doi.org/10.1016/j.polymdegradstab.2017.05.029
23. Liu Y, Shao J, Sun J, Bian X, Chen Z, Li G, Chen X (2015) Toughening effect of poly(d-lactide)-b-poly(butylene succinate)-b-poly(d-Lactide) copolymers on poly(l-Lactic Acid) by solution casting method. Mater Lett 155:94–96. https://doi.org/10.1016/j.matlet.2015.04.124
24. Vilay V, Mariatti M, Ahmad Z, Pasomsouk K, Todo M (2009) Characterization of the Mechanical and thermal properties and morphological behavior of biodegradable poly(l-lactide)/poly(e-caprolactone) and poly(l-lactide)/poly(butylene succinate-Co-l-lactate) polymeric blends. J Appl Polym Sci 114:1784–1792. https://doi.org/10.1002/app.30683
25. Srithep Y, Veang-In O, Pholharn D, Turng LS, Morris J (2021) Improving Polylactide toughness by plasticizing with low molecular weight polylactide-poly(butylene succinate) copolymer. J Renew Mater 9:1267–1281. https://doi.org/10.32604/jrm.2021.015604
26. Shibata M, Inoue Y, Miyoshi M (2006) Mechanical properties, morphology, and crystallization behavior of blends of poly (L-lactide) with poly (butylene succinate-Co-L-lactate) and poly (butylene succinate). Polymer (Guildf) 47:3557–3564
27. Zhang B, Bian X, Xiang S, Li G, Chen X (2017) Synthesis of PLLA-based block copolymers for improving melt strength and toughness of PLLA by in situ reactive blending. Polym Degrad Stab 136:58–70. https://doi.org/10.1016/j.polymdegradstab.2016.11.022
28. Liu TY, Huang D, Xu PY, Lu B, Wang GX, Zhen ZC, Ji J (2022) Biobased seawater-degradable poly(butylene succinate- l -lactide) copolyesters: exploration of degradation performance and degradation mechanism in natural seawater. ACS Sustain Chem Eng 10:3191–3202. https://doi.org/10.1021/acssuschemeng.1c07176
29. Tan L, Chen Y, Zhou W, Nie H, Li F, He X (2010) Novel poly (butylene succinate-co-lactic acid) copolyesters: synthesis, crystallization, and enzymatic degradation. Polym Degrad Stab 95:1920–1927
30. Jacobsen S, Degée P, Fritz HG, Dubois P, Jérôme R (1999) Polylactide (PLA)—a new way of production. Polym Eng Sci 39:1311–1319. https://doi.org/10.1002/pen.11518
31. Jacobsen, S.; Fritz, H.G.; Degée, P.; Dubois, P.; Jérôme, R. (2000) Continuous reactive extrusion polymerisation of L-lactide—an engineering view. In Proceedings of the Macromolecular Symposia; Wiley-VCH Verlag, 153: 261–273.
32. Jacobsen S, Fritz HG, Degée P, Dubois P, Jérôme R (2000) Single-step reactive extrusion of PLLA in a Corotating twin-screw extruder promoted by 2-ethylhexanoic acid tin(II) salt and triphenylphosphine. Polymer (Guildf) 41:3395–3403. https://doi.org/10.1016/S0032-3861(99)00507-8
33. Terzopoulou Z, Zamboulis A, Bikiaris DN, Valera MA, Mangas A (2021) Synthesis, properties, and enzymatic hydrolysis of poly(lactic acid)-co-poly(propylene adipate) block copolymers prepared by reactive extrusion. Polymers (Basel) 13:4121. https://doi.org/10.3390/polym13234121
34. Nishida M, Nishimura Y, Tanaka T, Oonishi M, Kanematsu W (2012) Solid state NMR analysis of poly(L-lactide) random copolymer with poly(ε-caprolactone) and its reactive extrusion process. J Appl Polym Sci 123:1865–1873. https://doi.org/10.1002/app.34674
35. Viamonte-Aristizábal S, García-Sancho A, Campos FMA, Martínez-Lao JA, Fernández I (2021) Synthesis of high molecular weight L-polylactic acid (PLA) by reactive extrusion at a pilot plant scale: influence of 1, 12-dodecanediol and Di (trimethylol propane) as initiators. Eur Polym J 161:110818
36. Klonos PA, Evangelopoulou A, Terzopoulou Z, Zamboulis A, Valera MÁ, Mangas A, Kyritsis A, Bikiaris DN (2022) Revisiting non-conventional crystallinity-induced effects on molecular mobility in sustainable diblock copolymers of poly(propylene adipate) and polylactide. Molecules 27:7449. https://doi.org/10.3390/molecules27217449
37. Klonos PA, Terzopoulou Z, Zamboulis A, Valera MÁ, Mangas A, Kyritsis A, Pissis P, Bikiaris DN (2022) Direct and Indirect effects on molecular mobility in renewable polylactide-poly(propylene adipate) block copolymers as studied via dielectric spectroscopy and calorimetry. Soft Matter 18:3725–3737. https://doi.org/10.1039/d2sm00261b
38. Degé PH, Dubois PH, Jacobsen S, Fritz HG, Jérome R (1999) Beneficial effect of triphenylphosphine on the bulk polymerization of L, L-lactide promoted by 2-ethyihexanoic acid tin (II) salt. J Polym Sci Part A Polym Chem 37:2413–2420
39. Pamies, R.; Hernández Cifre, J.G.; del Carmen López Martínez, M.; García de la Torre, J. (2008) Determination of Intrinsic Viscosities of Macromolecules and Nanoparticles. Comparison of Single-Point and Dilution Procedures. Colloid Polym. Sci, 286: 1223–1231 https://doi.org/10.1007/s00396-008-1902-2.
40. Huang J, Lisowski MS, Runt J, Hall ES, Kean RT, Buehler N, Lin JS (1998) Crystallization and microstructure of Poly (L-Lactide-Co-Meso-Lactide) copolymers. Am Chem Soc Polym Prepr Div Polym Chem 39:88–89. https://doi.org/10.1021/ma9714629
41. Oliver WC, Pharr GM (1992) An improved technique for determining hardness and elastic modulus using load and displacement sensing indentation experiments. J Mater Res 7:1564–1583. https://doi.org/10.1557/jmr.1992.1564
42. Tsongas K, Tzetzis D, Karantzalis A, Banias G, Exarchos D, Ahmadkhaniha D, Zanella C, Matikas T, Bochtis D (2019) Microstructural, surface topology and nanomechanical characterization of electrodeposited Ni-P/SiC nanocomposite coatings. Appl Sci 9:2901. https://doi.org/10.3390/app9142901
43. Mansour G, Tzetzis D (2013) Nanomechanical characterization of hybrid multiwall carbon nanotube and fumed silica epoxy nanocomposites. Polym—Plast Technol Eng 52:1054–1062. https://doi.org/10.1080/03602559.2013.769581

44. Mansour G, Tzetzis D, Bouzakis KD (2013) A Nanomechanical Approach on the measurement of the elastic properties of epoxy reinforced carbon nanotube nanocomposites. Tribol Ind 35:190–199
45. Grigora ME, Terzopoulou Z, Tsongas K, Bikiaris DN, Tzetzis D (2022) Physicochemical Characterization and finite element analysis-assisted mechanical behavior of polylactic acid-montmorillonite 3D printed nanocomposites. Nanomaterials 12:2641. https://doi.org/10.3390/nano12152641
46. Mansour G, Zoumaki M, Tsongas K, Tzetzis D (2021) Microstructural and finite element analysis—assisted nanomechanical characterization of maize starch nanocomposite films. Mater Res. https://doi.org/10.1590/1980-5373-MR-2020-0409
47. Kim BJ, White JL (2004) Engineering analysis of the reactive extrusion of E-caprolactone: the influence of processing on molecular degradation during reactive extrusion. J Appl Polym Sci 94:1007–1017
48. Sonseca A, El Fray M (2017) Enzymatic synthesis of an electrospinnable Poly(Butylene Succinate-Co-Dilinoleic Succinate) thermoplastic elastomer. RSC Adv 7:21258–21267. https://doi.org/10.1039/c7ra02509b
49. Velmathi S, Nagahata R, Sugiyama JI, Takeuchi K (2005) A rapid eco-friendly synthesis of Poly(Butylene Succinate) by a direct polyesterification under microwave irradiation. Macromol Rapid Commun 26:1163–1167. https://doi.org/10.1002/marc.200500176
50. Neibolts N, Platnieks O, Gaidukovs S, Barkane A, Thakur VK, Filipova I, Mihai G, Zelca Z, Yamaguchi K, Enachescu M (2020) Needle-free electrospinning of nanofibrillated cellulose and graphene nanoplatelets based sustainable Poly (Butylene Succinate) nanofibers. Mater Today Chem 17:100301. https://doi.org/10.1016/j.mtchem.2020.100301
51. Siracusa V, Lotti N, Munari A, Dalla Rosa M (2015) Poly(Butylene Succinate) and Poly(Butylene Succinate-Co-Adipate) for food packaging applications: gas barrier properties after stressed treatments. Polym Degrad Stab 119:35–45. https://doi.org/10.1016/j.polymdegradstab.2015.04.026
52. Papageorgiou GZ, Bikiaris DN (2005) Crystallization and melting behavior of three biodegradable Poly(Alkylene Succinates). A comparative study. Polymer (Guildf) 46:12081–12092. https://doi.org/10.1016/j.polymer.2005.10.073
53. Qiu Z, Fujinami S, Komura M, Nakajima K, Ikehara T, Nishi T (2004) Nonisothermal crystallization kinetics of Poly (Butylene Succinate) and Poly (Ethylene Succinate). Polym J 36:642–646
54. Ba C, Yang J, Hao Q, Liu X, Cao A (2003) Syntheses and physical characterization of new aliphatic triblock Poly(L-Lactide-b-Butylene Succinate-b-L-Lactide)s bearing soft and hard biodegradable building blocks. Biomacromol 4:1827–1834. https://doi.org/10.1021/bm034235p
55. Michler GH, Baltá-Calleja FJ, Adhikari R, Knoll K (2003) Microindentation hardness of SB-Block copolymers relating to nano-mechanical mechanisms. J Mater Sci 38:4713–4723. https://doi.org/10.1023/A:1027418801020